

Chapter VI

Adsorption Studies Employing Nanocomposites

Carbon composites with metals/ metal oxides/ metal salts as dopants, especially to nanosize have found their applications in various diverse fields. These materials having magnetic nano metal composites/ metal oxides possess a relatively high surface area, small particle size and porous nature, in turn enhancing the adsorption capacity towards organic and inorganic wastewaters. Magnetic nanocomposites have contributed in the sequestration of dyes due to their astounding significance in accelerating separation rate and improvising its efficiency to trap molecules of interest¹⁷⁷.

Commercially available magnetic particles are expensive, therefore, the chosen ecofriendly materials (PJBAC and GDAC) are subjected to magnetic modification. Sorption performances of the newly synthesized magnetic nanocomposites are dealt in this chapter.

6.1 Characterisation of PJBAC-CFC/ GDAC-CFC

6.1.1 SEM/ EDAX Analyses

SEM images of the unloaded PJBAC-CFC and GDAC-CFC shown in figures 6.1 and 6.2 imply the presence of numerous pores with irregular sizes, suitable for dye sequestration. In spite of the composites surfaces being covered by small aggregates of cobalt ferrite, a porous nature is seen leftover, referring to its high adsorbable properties. EDAX spectra depicted in figures 6.3 and 6.4 confirm the presence of Co, Fe and O elements in the framework of the composites.

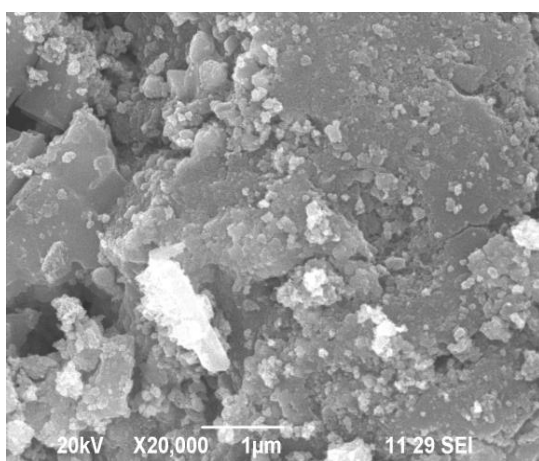


Figure 6.1 SEM Image - PJBAC-CFC

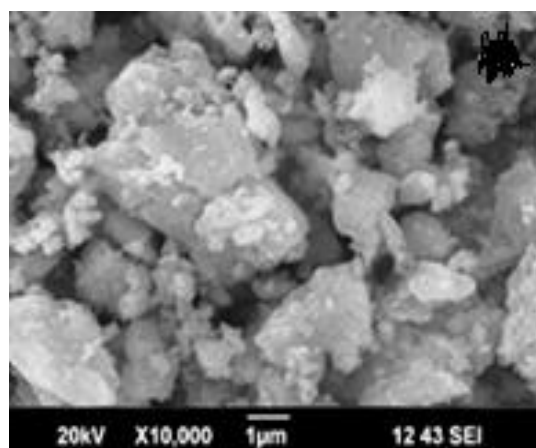


Figure 6.2 SEM Image - GDAC-CFC

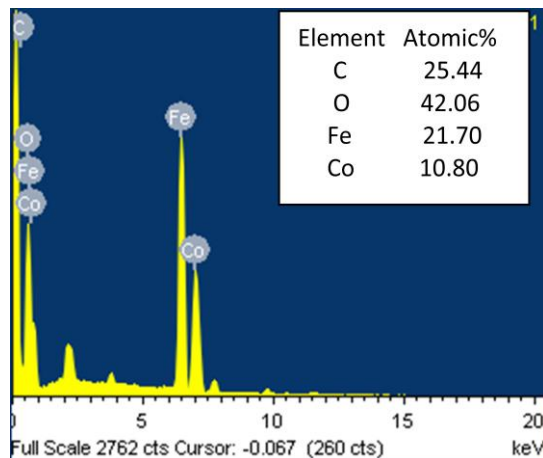


Figure 6.3 EDAX Spectrum- PJBAC-CFC

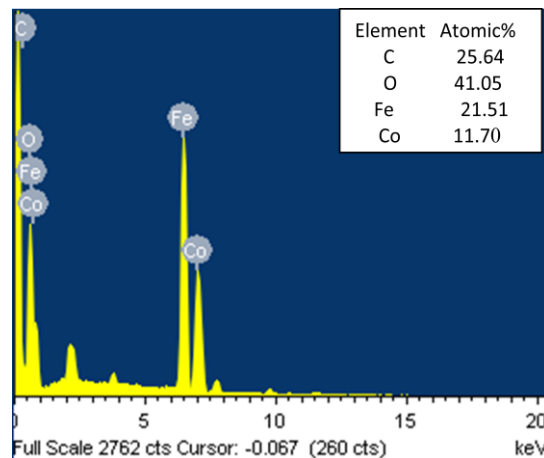


Figure 6.4 EDAX Spectrum GDAC-CFC

6.1.2 X-Ray Diffraction Studies

High purity and crystallinity of the samples were analysed by X-ray Powder Diffraction technique using Advance X-Ray Diffractometer (XPERT-PRO, Bruker AXS D8) X-ray diffraction patterns of PJBAC/GDAC, CoFe_2O_4 and CoFe_2O_4 doped PJBAC/GDAC are illustrated in figures 6.5 and 6.6 respectively. Appearance of peaks at $2\theta = 26.5^\circ$ (a) corresponds to presence of carbon in PJBAC/GDAC. The diffraction peaks (c) indexed at (220), (311), (400), (511), (440) matches with the cubic spinel structure (JCPDS card no. 22-1086) of cobalt ferrite (b), supporting the formation of a single phase spinel (CoFe_2O_4). The average crystalline sizes of CoFe_2O_4 doped PJBAC/GDAC materials were calculated using Scherrer's equation (26) and recorded as 20 nm/10 nm for PJBAC/GDAC magnetized materials respectively.

$$D = \frac{0.9\lambda}{\beta \cos\theta} \quad (26)$$

where

D = average crystalline diameter

k = constant (0.9 for $\text{Cu-K}\alpha$)

λ = X-ray wavelength (0.15405 nm for $\text{Cu-K}\alpha$)

β = peak width of half maximum of XRD diffraction lines

θ = Bragg's diffraction angle in degree.

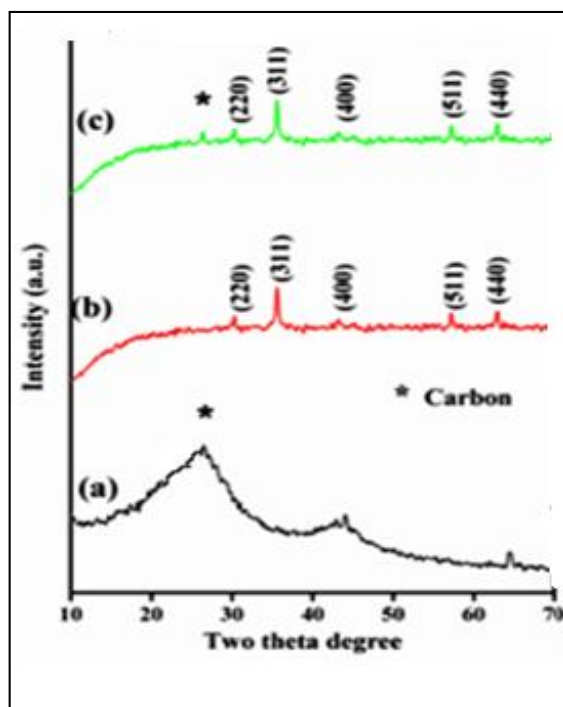


Figure 6.5 XRD Patterns of (a) PJBAC (b) CoFe_2O_4 and (c) Cobalt Ferrite Doped PJBAC

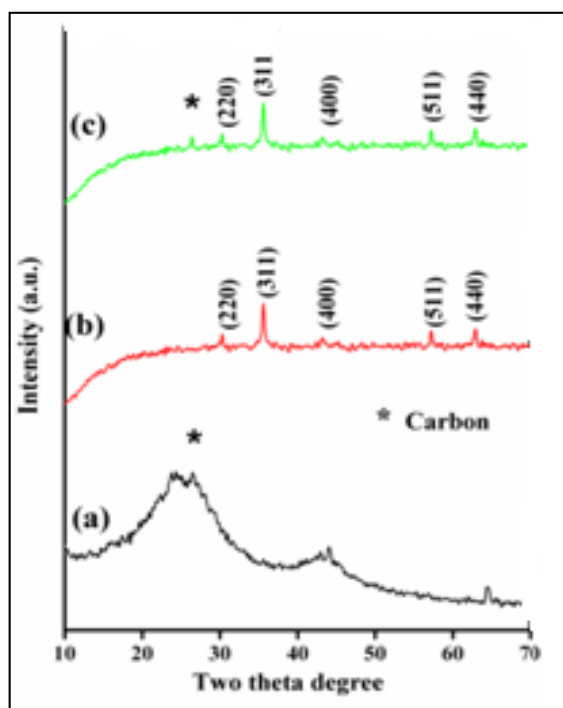


Figure 6.6 XRD Patterns of (a) GDAC (b) CoFe_2O_4 and (c) Cobalt Ferrite Doped GDAC

6.1.3 Atomic Force Microscopic Analysis.

Particle size of the composite was visualised using Atomic Force Microscope, NTMDT (NTEGRA PRIMA) model. The nanosize nature of PJBAC/GDAC-CFC materials as derived from AFM studies are represented in figures (6.7-6.10). Clarity in the 3D peaks of surface topography images is favoured by the presence of sharp peaks at 20 nm and 1.4 nm respectively for plant and animal derived carbons, emphasizing the nanosize of the composites.

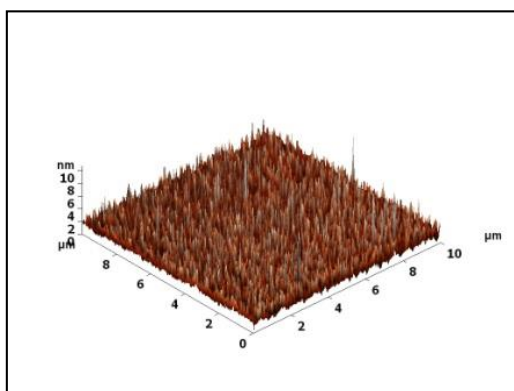


Figure 6.7 Surface Topography of PJBAC-CFC

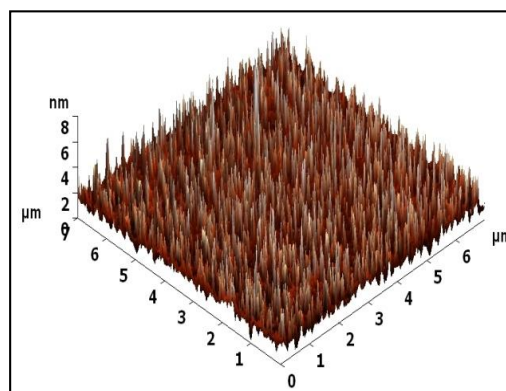


Figure 6.8 Surface Topography of GDAC-CFC

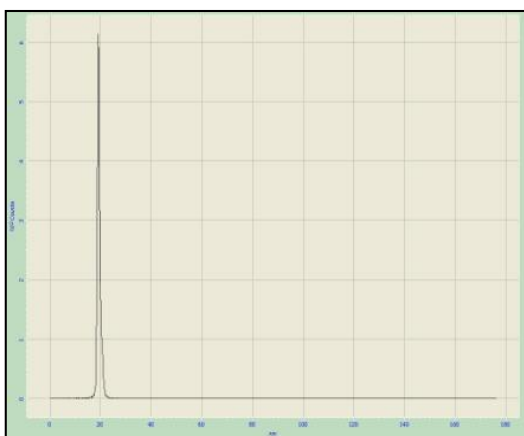


Figure 6.9 Histogram of PJBAC-CFC

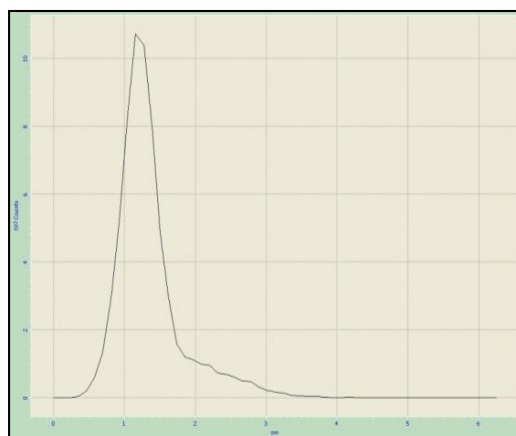


Figure 6.10 Histogram of GDAC-CFC

6.1.4 BET Surface Area

BET surface areas and pore volumes of the carbon precursors and their composites are listed in Table 6.1, wherein the parametric values are found to diminish in composites. The relatively large surface area and high pore volume of the former, show that the pores were not completely blocked by magnetic CoFe_2O_4 and thus the composite is classified as a porous material with good adsorption capacity, coinciding with SEM images. Similar observation had been made in the case of magnetic oxide-supported activated carbon^{178,179}.

6.1.5 Magnetic Properties

The magnetic particles with sizes lesser than 30 nm exhibit super paramagnetism property, this responds well to the magnetic fields without any permanent magnetization¹⁸⁰. In the present study, the paramagnetic properties of the synthesized magnetic nanocomposites were verified using Vibrating Sample Magnetometer (Lakeshore VSM 7410) at room temperature and measuring the obtained magnetization curves. The results (Table 6.1) of high saturation magnetization (M_s) and coercivity (H_c) values are derived from the typical hysteresis loops (figures 6.11-6.12). Saturation magnetization readings of the magnetic nanocomposites being lesser than that reported for CoFe_2O_4 (86.1 emu/g) favour the attainment of magnetisation in the prepared carbons. Therefore, these samples with higher saturation magnetisation values responded to an external magnetic field, supporting the enhancement in their adsorption capacity. Confirmation of the magnetic separability by prepared composites were done by placing a magnet near a glass bottle filled with aqueous DB2 dye solution of 100 mg/L concentration and 60 mg PJBAC-CFC. The solution appearing black, turbid resulted in a clear solution (Figure 6.13).

Table 6.1 Surface Characterisation and Saturation Magnetization

Samples	BET-surface area (m^2g^{-1})	Total pore volume (cm^3g^{-1})	Saturation magnetization (emug^{-1})
PJBAC	385.2	0.132	0
PJBAC - CFC	208.4	0.351	32.1
GDAC	253.8	0.495	0
GDAC - CFC	129.1	0.283	26.7

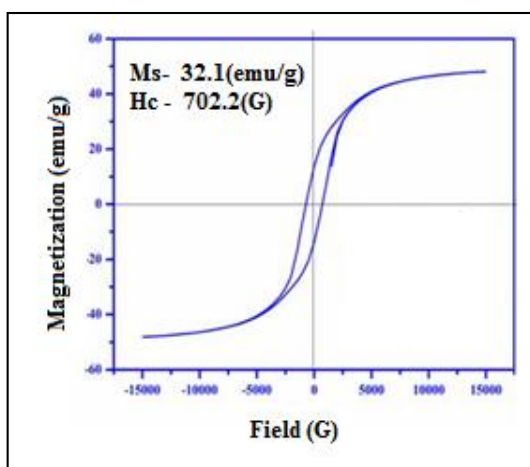


Figure 6.11 Magnetic Hysteresis Loops of PJBAC-CFC

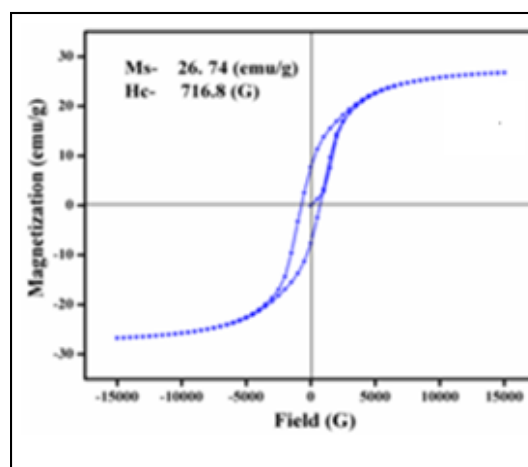


Figure 6.12 Magnetic Hysteresis Loops of GDAC-CFC

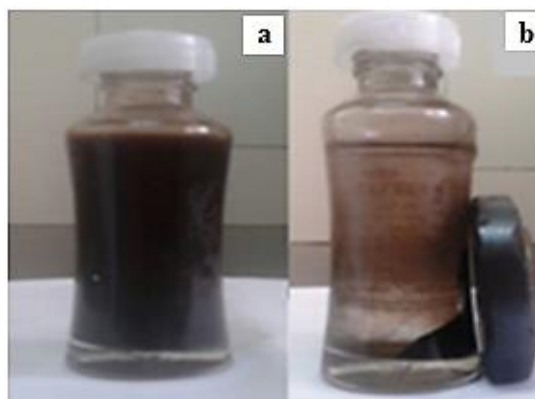


Figure 6.13 (a) Aqueous Dye Solutions with Magnetic Nanocomposites, (b) Dispersed Aqueous Dye Solutions under an External Magnetic Field

6.2 Batch Studies

The sorption nature of PJBAC-CFC/GDAC-CFC were experimentally verified through batch mode by the doses between 25 mg to 250 mg of at an initial concentration of 100 mg/L of DB2 agitated for 60 minutes. Since DB2 removal was pronounced with the carbon precursors, magnetic studies were limited to DB2 dye solutions. After the contact period, the supernatant was filtered and the residual concentrations were analyzed using UV-Visible Spectrophotometer. Figures 6.14 and 6.15 indicate the pronounced effect of the nano particles against their activated counterparts (Table 6.2). Maximum removal of DB2 had occurred at 60 mg of PJBAC-CFC and 100mg of GDAC-CFC against the requirement of 100 mg and 150 mg of PJBAC and GDAC.

Table 6.2 Comparison of Nano Magnetic Composites with Activated Carbon on DB2 Removal

Mass of adsorbent (mg)	Percentage Removal (DB2)			
	PJBAC	(PJBAC-CFMC)	GDAC	(GDAC-CFMC)
25	52.5	77.8	50.1	75.6
60	68.1	98.7	71.6	94.2
100	90.4	96.5	83.4	93.9
150	85.5	95.2	91.8	93.7

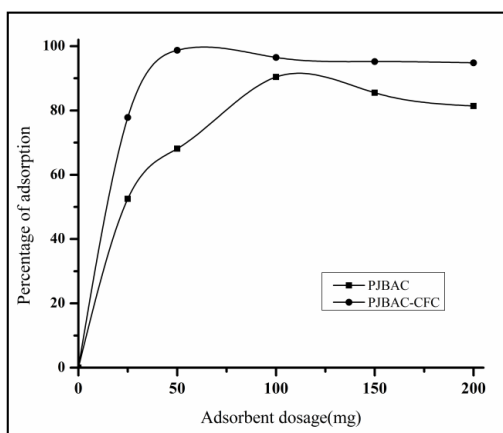


Figure 6.14 Effect of PJBAC- CFC on DB2 Removal

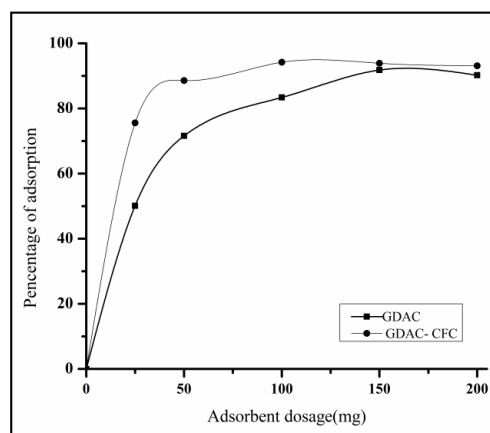


Figure 6.15 Effect of GDAC- CFC on DB2 Removal

6.3 Nano Photocatalytic Composite

Titanium dioxide possessing unique photocatalytic properties is capable of oxidizing organic compounds to carbon dioxide and water. Besides this significant quality which promotes its applications in waste water treatment. Titanium dioxide gets agglomerated when utilized in advanced oxidation process, sparing its separation from water¹⁸¹. The solution to this problem is focussed on doping TiO₂ with metal / non metal ions, where the non-metal doped catalysts had a significant influence under solar light irradiation¹⁸². Thus the prepared activated carbons, apart from being employed for adsorption process, their photo degradation property along with TiO₂ had been investigated^{183,184}. Also, the doping process upon TiO₂ promotes this applicability as cost effective, alternate against expensive TiO₂.

6.4. Characterisation of PJBAC-TiO₂ and GDAC-TiO₂

6.4.1 SEM/ EDAX

SEM images of PJBAC-TiO₂ and GDAC-TiO₂ (Figures 6.16-6.17) reveal the extensive dispersion of TiO₂ particles on the surface of activated carbons. Appearance of whitish aggregates in the images relates to the TiO₂ particles, which is insignificantly altering the surface area of the carbon precursors, justifying the photocatalytic degradation properties.

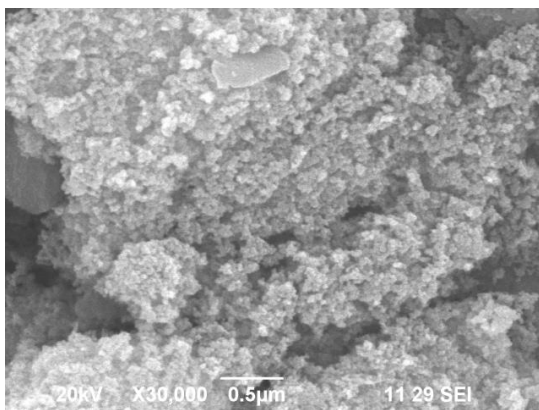


Figure 6.16 SEM Image of PJBAC-TiO₂

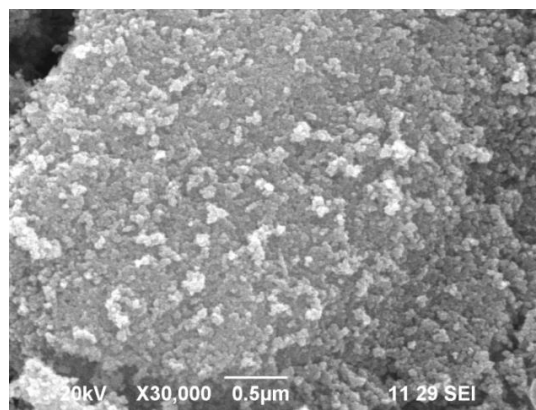


Figure 6.17 SEM Image of GDAC-TiO₂

Energy dispersive X-Ray spectra of photocatalytic composites (Figures 6.18-6.19) insist the presence of new peak at 1 and 8 keV corresponding to TiO₂.

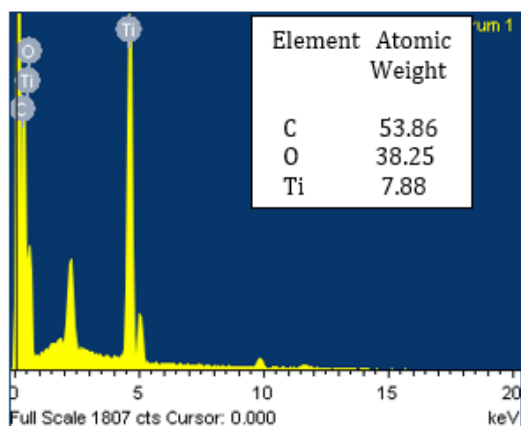


Figure 6.18 EDAX Spectra- PJBAC-TiO₂

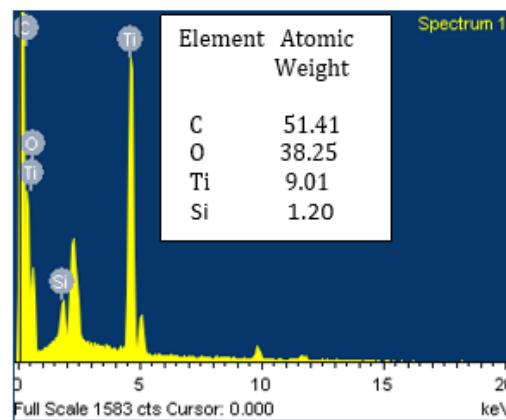


Figure 6.19 EDAX Spectra-GDAC-TiO₂

6.4.2 XRD analysis

The composites derived from the addition of TiO₂ to PJBAC/GDAC as per the experimental procedure dealt in chapter III, were examined using X-ray powder diffraction spectrometer. The XRD patterns of PJBAC-TiO₂ and GDAC-TiO₂ at figures 6.20-6.21 exhibit peaks at various diffractions of $2\theta = 25.5, 48.3, 54.5, 62.9$ corresponding to the (101),(200),(105) and (103) planes of anatase type matching with JCPDS No. 21-1272. The peaks at $2\theta = 27.7, 36.5, 38.1, 69.1$ being assigned to (001), (021), (210), (220) replicates the rutile phase of TiO₂. The crystalline sizes were calculated using equation 26, reflected 16 nm and 22 nm for PJBAC-TiO₂ and GDAC-TiO₂ which confirm the nanosize of the samples.

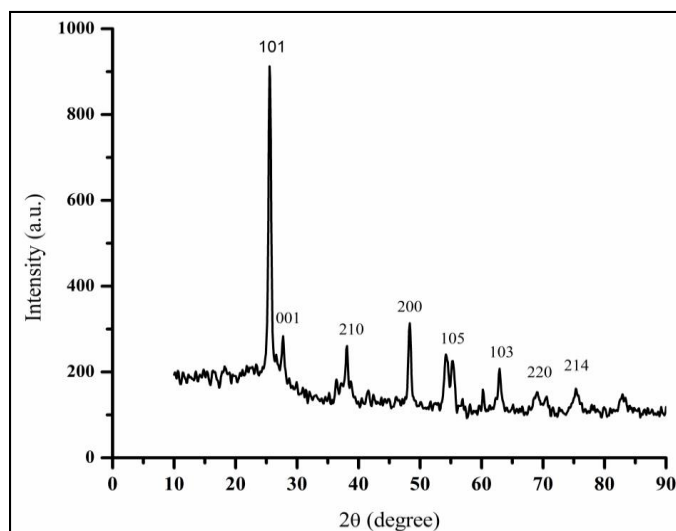


Figure 6.20 XRD Pattern of PJBAC-TiO₂

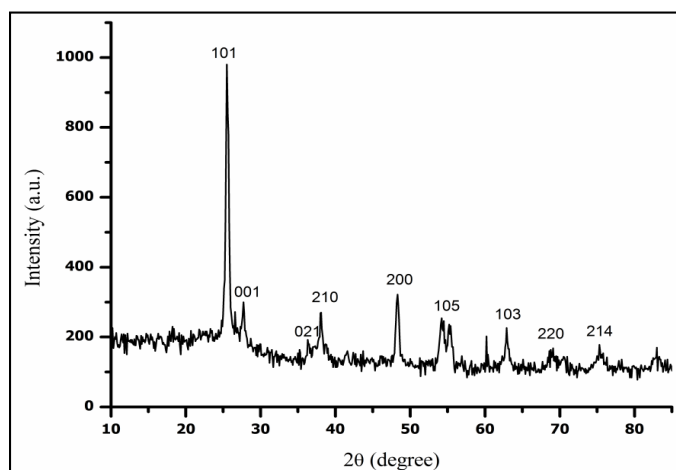


Figure 6.21 XRD Pattern of GDAC-TiO₂

6.5 Photocatalytic Degradation Studies

The photocatalytic efficiencies of the synthesized PJBAC-TiO₂ and GDAC-TiO₂ composites were explored by degrading the aqueous slurry of DB2 using batch visible-light photo reactor (Figure 6.22). The reactor comprises of six cylindrical pyrex glass tubes as sample holders with 150 mL capacity. The length and width of the sample holders are fixed as 30 cm × 2 cm. The entire set up is maintained at a temperature in the range of 25-30°C through water circulation. The visible-light source employed for a photoreaction is a 300W mercury lamp polished with anodized aluminium reflectors.

The light source is placed at the centre of the reactor circularly surrounded by the sample holders at a distance of 6 cm. This lamp emits light predominantly in the visible region at a wavelength above 410 nm with an intensity of $17\text{mW}/\text{cm}^2$.

In a typical procedure, varying doses of (50-250 mg) of the each composite was added to 100 mL of DB2 solution with the initial concentration of 100 mg/L in a glass tube followed by irradiation. 5 ml of sample was withdrawn from the reaction mixture at every 30th minute, upto 240 minutes (optimized condition) and analysed using UV-Visible spectrophotometer at a wavelength of 540 nm. The percentage removal of DB2 calculated as reported in earlier in batch process is shown in Table 6.3.

HPLC analysis was performed on ZORBAX SBC $185\ \mu\text{m}$, 150 mm x 10 mm column. The mobile phase and eluent was acetonitrile /water in the ratio of 60:40. The flow rate was 1 mL/min and the absorbance was recorded at 540 nm.

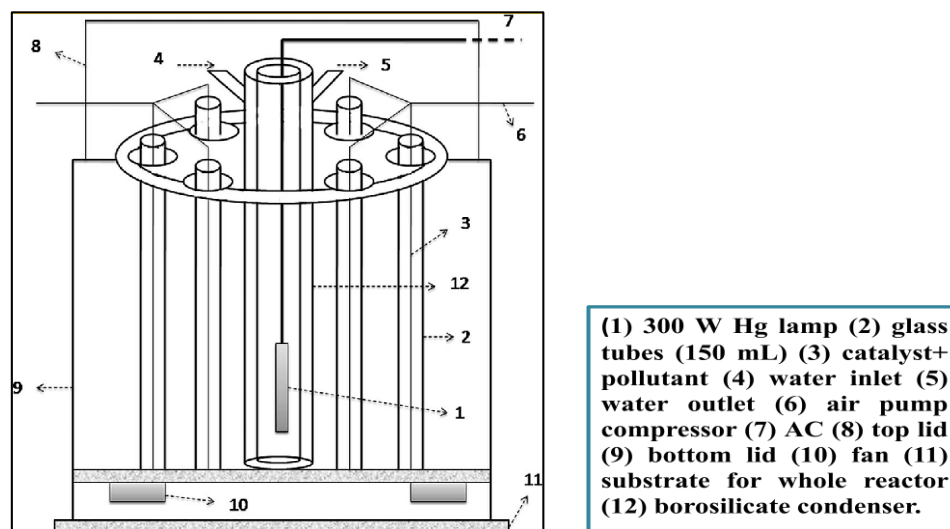


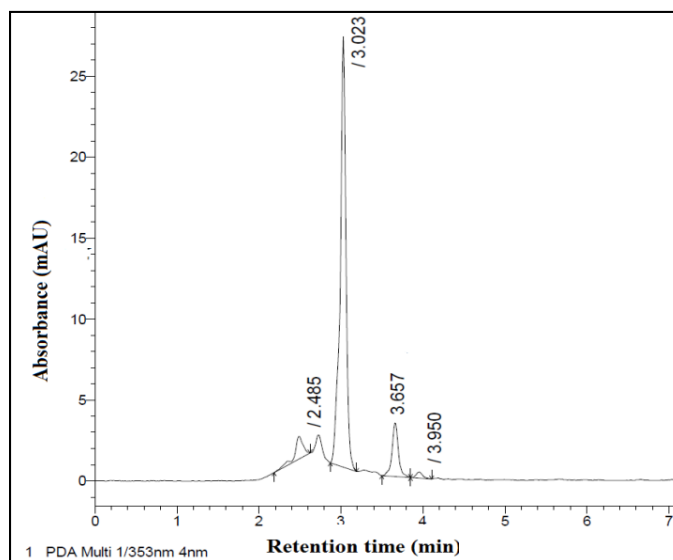
Figure 6.22 Photo Reactor

Table 6.3 Effect of Composites Doses on Percentage Removal of DB2

Contact time (min)	Dye Concentration(mg/L)	Composite doses (mg)	% Removal of DB2	
			PJBAC-TiO ₂	GDAC-TiO ₂
240	100	50	23.2	18.4
		100	48.4	39.5
		150	65.9	58.2
		200	86.8	80.9
		250	87.2	81.8

6.6 HPLC Analysis

The photo degradation of DB2 samples using PJBAC-TiO₂ and GDAC-TiO₂ were confirmed by analysing the samples using HPLC (Agilent 1100 series) equipped with auto sampler. Figures 6.23 -6.25 sketch out the chromatograms of aqueous DB2 solution and their corresponding degraded samples. Reduction peak heights 7.6 mAU and 15.0 mAU for PJBAC-TiO₂ and GDAC-TiO₂ treated DB2 samples against the peak height of 28.0 mAU in aqueous DB2 solution confirms that the degradation had occurred.

**Figure 6.23 HPLC chromatogram-DB2**

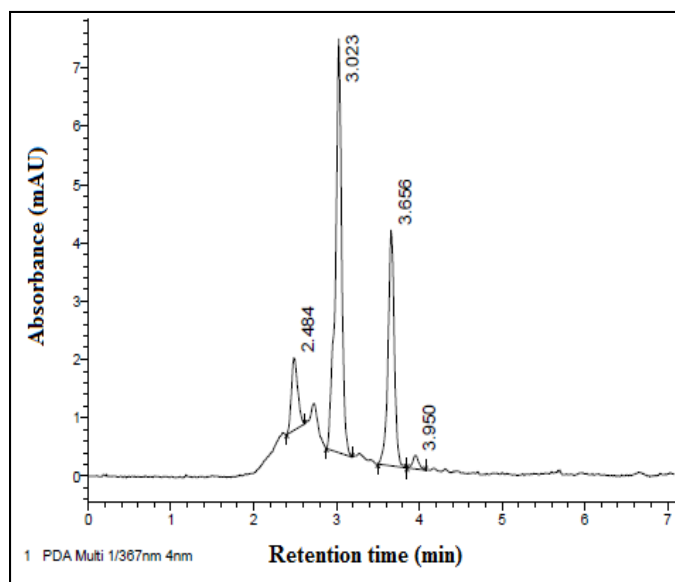


Figure 6.24 HPLC Chromotogram- DB2 - Photodegradation by PJBAC-TiO₂

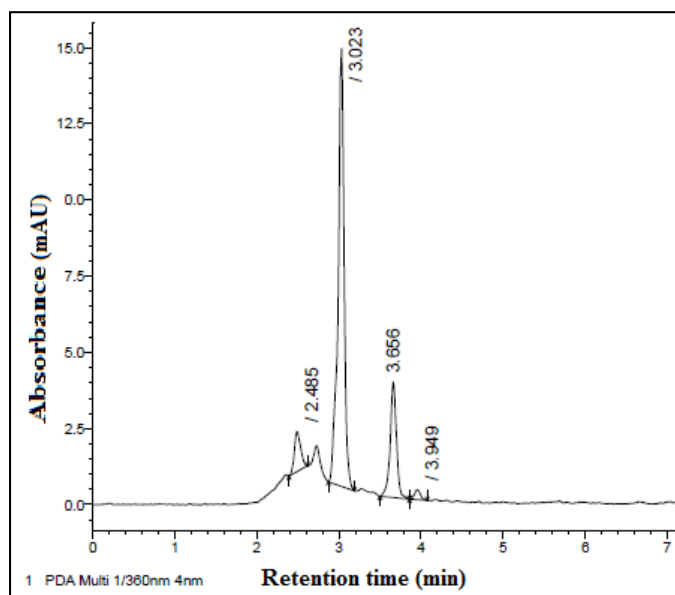


Figure 6.25 HPLC Chromotogram - DB2 - Photodegradation by GDAC-TiO₂